LONGITUDINAL DISPERSION AND TRACER MIGRATION IN A RADIAL FLOW FIELD

František Majs and John C. Seaman

AUTHORS: Soil Scientists, Savannah River Ecology Laboratory, The University of Georgia, Drawer E, Aiken, SC 29802
REFERENCE: *Proceedings of the 2007 Georgia Water Resources Conference*, held March 27–29, 2007, at the University of Georgia.

Abstract. Hydrodynamic dispersion is an important factor controlling contaminant migration in the subsurface environment. However, few comprehensive data sets exist for evaluating the impact of travel distance and site heterogeneity on solute dispersion under non-uniform flow conditions. In addition, anionic tracers are often used to estimate physical transport parameters based on an erroneous assumption of conservative (i.e., non-reactive) behavior. Therefore, a series of field experiments using tritiated (^{3}H) water and other commonly used hydrologic tracers, bromide (Br) and fluorinate benzoic acid (FBA), were conducted to evaluate solute transport processes in a diverging axisymmetric flow field. Tracer migration was monitored using a set of six, multilevel sampling wells concentrically spaced at distances from 2.0 to 4.5 meters around the injection well. Soil hydraulic parameters for aquifer matrix were inversely optimized and an average longitudinal dispersivity for ^{3}H breakthrough was estimated using numerical finite-element code (i.e., HYDRUS-2D) capable of describing an axisymmetric diverging flow. Tremendous variation in tracer arrival times between similar sampling locations and multiple arrival peaks observed for some sampling locations were observed for both, ^{3}H and Br. Migration of the Br was retarded, when compared to that of the ^{3}H, and analysis of the anion data assuming conservative behavior would thus yield higher dispersivity values than conservative tracer.

INTRODUCTION

An estimate of hydraulic conductivity and field-scale dispersivity is crucial for predicting contaminant plume migration in groundwater. Dispersion arises from a tortuous flow path caused by hydraulic heterogeneity of the aquifer matrix and diffusive properties of the solute in groundwater (Welty and Gelhar, 1994). An agreement among researchers prevails with regards to the scale dependence of the dispersivity. Dispersivity increases with distance until it reaches an asymptotic value by averaging out heterogeneities of aquifer matrix with distance (Gelhar et al., 1992). If valid, a single, asymptotic dispersivity value greatly simplifies interpretation of experimental results.

Most field-scale experiments impose an axisymmetric flow field, with converging/diverging flow induced by groundwater pumping/injection, respectively. This results in a non-uniform flow field, where flow rates change with the distance from the well, as opposed to uniform flow, where flow rates stay constant (Neuweiler et al., 2001). During the initial step of an injection experiment, steady-state flow conditions under forced gradient are established by injecting/pumping non-labeled water. In most cases, a known volume of tracer labeled water is injected afterwards at the same, steady flow rate, and then switched back to the non-labeled water, to spread the tracer solution out into the aquifer. Prolonged travel distances violate the assumption of gradual mixing of tracer over sufficient amount of time along the assumed velocity vectors, because these tend to be assessed erroneously. Velocity is actually larger than the assumed velocity due to the longer path that the tracer ought to travel between point A and B.

Tracers such as chloride and bromide have been widely used as conservative tracers for evaluating the physical processes associated with subsurface migration. The assumption of conservative behavior is based on the aquifer's matrix mineralogy dominated by clay minerals that bear net-negative charge, do not sorb and can even repel tracer anions. This repulsion can actually result, in some instances, in an early arrival of anionic tracers when compared to tritium, a true conservative tracer (Melamed et al., 1994). The opposite has been observed; however, in laboratory and field experiments conducted with soils and sediments dominated by significant quantities of iron and aluminum oxides (Seaman, 1998).

Objectives

Models describing uniform, one-dimensional flow, even though inappropriate, are frequently used to interpret data from axisymmetric flow experiments. These improperly applied models, with an inherent weakness of a constant dispersivity value in governing equation, introduce an uncertainty with regards to the accuracy of prediction of contaminant migration (Welty and Gelhar, 1994). The main objective of this paper is to optimize soil hydraulic and solute transport parameters for the interpretation of axisymmetric field-scale experiment.

Table 1. Summary of Tracer Pulse Composition and Duration for the Two Injection Experiments

Pulse	A	B
Volume (L)	15,120	31,752
Duration (min)	256	560
Composition	2,000 pCi mL^{-1} ^3H	like A + 0.003 *M* Br as KBr and $CaBr_2$

MATERIALS AND METHODS

Test Site Description

The Injection Test Site (ITS) was constructed within the highly-weathered, coarse-textured sediments of the Atlantic Coastal Plain underlying The Department of Energy's Savannah River Site (SRS) near Aiken, SC (Seaman et al., 2006a and 2007). The aquifer consists predominantly of sands and clayey sand with clay, sandy clay, and gravel lenses (WSRC, 1992). The depth of the documented continuous impermeable clay layer is 23.2 m, isolating the upper test aquifer from the underlying aquifer and restricting the depth of the experimental domain. The ITS consisted of a 0.15-m ID and 19.2-m deep central injection well (IW), screened over a 4.56-m interval starting at the depth of 13.5 m, and six 0.075-m ID concentrically spaced observation wells (S1 to S6) at approximate distances of 2, 3, and 4.5 m. The six observation wells were screened (0.15 m) in three distinct zones in depths at 12.5, 14.6, and 16.8 m for the total of eighteen distinct sampling locations (Seaman et al., 2006a).

Injection Experiments

Both experiments consisted of injecting non-labeled groundwater through the IW for approximately 24 hours at a rate of 56.7 L min^{-1} to establish a steady, forced diverging gradient. Two injection experiments, A and B, were conducted (Table 1). After each experiment the non-labeled water was applied at the same rate, to spread the tracer solution pulse out. Water levels were recorded periodically for each well and samples were collected at each sampling location by continuous pumping at a rate of ≈0.1 L min^{-1} throughout the course of the tracer experiment. The tritium (^3H) and bromide (Br) concentrations of the groundwater samples were analyzed by liquid scintillation and ion chromatography with UV/Vis detection, respectively (Seaman, 1998).

Table 2. Optimized van Genuchten (1980) Hydraulic Parameters for Material 3 – Aquifer Matrix

θr	θs	Alpha	n	Ks
m^3 m^{-3}	m^3 m^{-3}	m^{-1}		m day^{-1}
0.04545	0.392	5.5842	2.0811	5.0074

Transport Model

Tracer transport calculations were made using the HYDRUS-2D numerical finite-element code (Šimůnek et al., 1999). The Richards equation and the physical equilibrium convection-dispersion equation were used as governing equations. HYDRUS-2D also allows for inverse optimization of parameters with implemented Levenberg-Marquardt nonlinear weighing scheme that minimize differences between observed and predicted values.

The axisymmetric flow domain with radius of 30 m and depth of 23.2 m consists of four materials. Sand filter and bentonite seal of the borehole and the native aquifer sediment were represented by material 1, 2, and 3, respectively. Material 4 was added after the preliminary run, representing the volume between sand filter and aquifer sediment, because of the inability to simulate the steep hydraulic gradient observed in the field. It has been documented previously that prolonged injection can lead to a decrease in saturated hydraulic conductivity (Ks) near the well due fouling with dissolved salts and dispersed colloids. The bottom of the flow domain was treated as a no-flow boundary, due to the low Ks of the clay layer. The same water flow boundary type was assigned to the soil surface and the non-screened portion of the well, whereas the screened interval of the IW was treated as a constant flow boundary with 25 nodes. The side opposed to the axis of symmetry was treated as a constant pressure boundary with groundwater table fixed at 12.2 m.

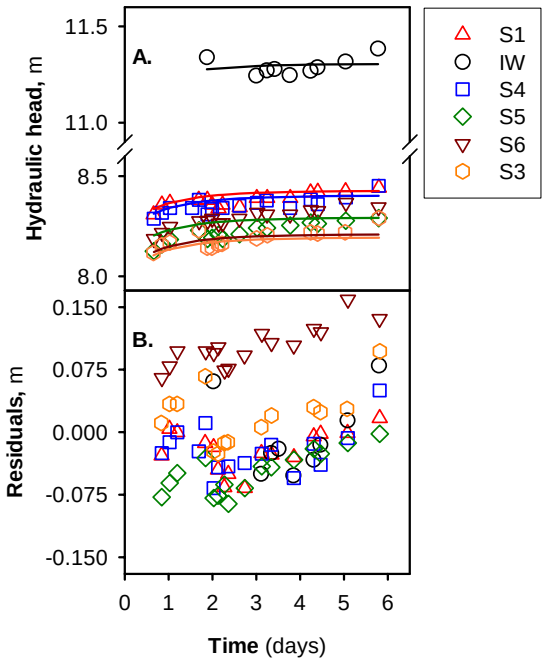

Figure 1. Observed hydraulic heads plotted for five of the six monitoring wells (S1 - S6) and an injection well (IW) with inversely optimized hydraulic head, color lines (A), and appropriate residuals (B).

Inverse Optimization of Parameters

Soil Hydraulic Parameters. Hydraulic properties for materials 1 and 2 were assigned default values for appropriate texture class by Rosetta DLL, an independent pedotransfer function code coupled with HYDRUS code, and were not optimized (Schaap et al., 2001). Material 3, aquifer sediment, parameter estimates were based on a previous study by Looney et al. (1987) and were included in inverse optimization. All Material 4 properties were initially identical to Material 3 and only Ks was gradually lowered to match the steep hydraulic gradient recorded in the field (Fig. 1). Measured groundwater table levels were given the same weight, assigned location at the proper radial distance from the IW, and treated as a pressure head measurements.

Solute Transport Parameters. Steady flow conditions were imported from the previous step with the optimized van Genuchten's (1980) soil hydraulic parameters. Default values of 1.6 g cm^{-3} were used for bulk densities of all materials, because no data or estimates exist. Measured relative ^3H concentrations from the experiment A were given the same weight, assigned a proper sampling location, and treated as concentration measurements. Longitudinal dispersivities (α_L) of all four materials were subject to optimization, allowed to vary between 0.01 and 2 m, and transverse dispersivities were fixed at a fraction of the α_L value. Measured ^3H and Br concentrations from the experiment B, were compared to the predicted ^3H curves, using model parameters calibrated in the experiment A.

RESULTS

Soil Hydraulic Parameters

Optimized hydraulic parameters for Material 3, aquifer sediment, are summarized in Table 2. Saturated hydraulic conductivity (Ks) was the only unique parameter, as characterized by relatively small standard error (SE) and tight 95% confidence interval (CI) (Table 3). Despite favorable statistics for optimized Ks, an effort was made to eliminate a systematic bias observed in the plot of residuals by linearly increasing weighting of later pressure head measurements (Fig. 1). However, bias was eliminated only partially. Statistics for the rest of the parameters were dominated by a large SE's and very wide, physically unrealistic CI's (data not shown). Field estimate of Ks for the native aquifer sediment was 7.6 and the optimized value was 5.0 m day^{-1}. Large differences between estimated and numerically optimized values illustrate the complexity of solute migration in a close proximity to the point of release. The ability to separate the partial contributions of the individual materials to the mean Ks of the flow domain is a unique property of finite element model. Separating part of the flow domain, whose properties were changed (i.e., addition of new materials) or merely affected by well installation (e.g., smearing of the borehole wall during drilling), can greatly change flow patterns for the entire domain. Altered flow patterns inadvertently change the assumed velocity vectors and the assumption of the gradual mixing of the tracer.

Solute Transport Parameters

The contribution of individual materials to the overall hydrodynamic dispersion of the tritium (^3H) in experiment A is variable. Values of the longitudinal dispersivity (α_L) for sand and low conductivity zone were at the minimum and that of the bentonite at the maximum allowed, 0.01 and 2 m, respectively. Uniqueness of the optimized values is questionable, because SE's for materials 1, 2, and 4 are multiples of the optimized values and predicted CI's indicate physically unrealistic conditions (data not shown). The optimized value of α_L for aquifer sediment is 0.96 m with SE of ≈0.31, approximately ⅓ of the optimized α_L, and physically realistic CI (Table 3). Very similar values and statistics were derived from several optimization runs with different initial parameters.

Axisymmetric approximation with constant α_L generally described ^3H behavior at the wells closest to the IW. Complex ^3H breakthrough patterns at the wells further from the IW did not allow for any further generalization because α_L would have been generally under-predicted at the deeper sampling locations 1 and 2, and over-predicted at the top (Fig. 2). In general, bromide (Br) demonstrated retardation, which increased travel times and would increase optimized α_L values, when compared to the conservative tracer, ^3H (Fig. 2). Early breakthrough of the Br, most likely because of the local mineralogical heterogeneities, is also visible at further distances from the IW, wells S5 and S6. Demonstrated retardation and erratic breakthrough patterns of Br would greatly violate the conservative behavior assumption (Seaman et al., 2006b).

Table 3. Optimized Saturated Hydraulic Conductivity (Ks) and Longitudinal Dispersivity (α_L) for Material 3, Aquifer Matrix, Using Measured Water Levels and Measured Tritium Concentrations for Pulse A

Variable	Value	SE	95% Conf. Int.	
			Lower	Upper
Ks (m day^{-1})	5.0074	0.0003924	5.0066	5.0082
α_L (m)	0.9598	0.30716	0.3565	1.5631

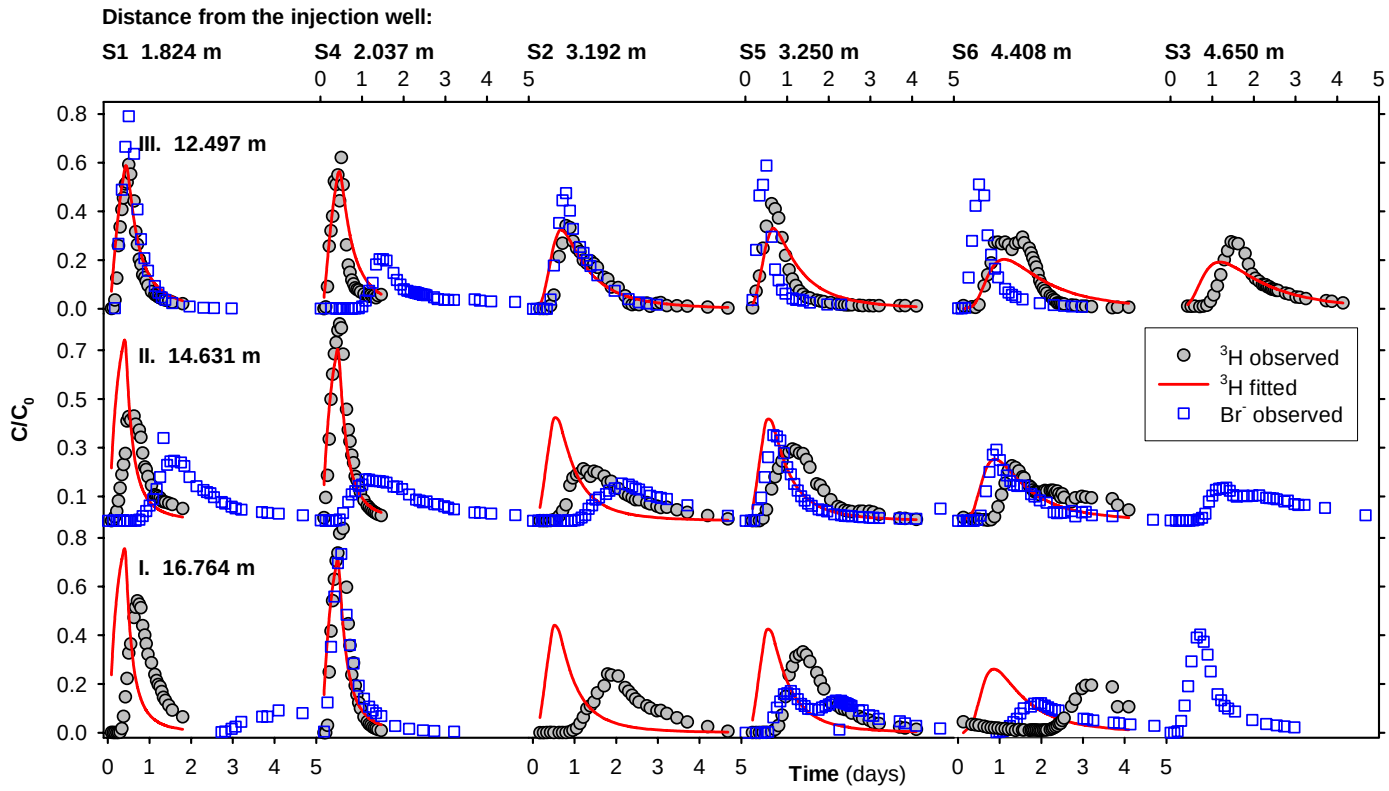

Figure 2. Tritium (^{3}H) and bromide (Br) concentrations for the experiment B plotted together with ^{3}H optimized curves using inversely fitted van Genuchten's (1980) soil hydraulic parameters and longitudinal dispersivity from the experiment A. Data are plotted over time for six observation wells, S1 thru 6, concentrically spaced around the injection well.

LITERATURE CITED

Gelhar, L.W., C. Welty and K.R. Rehfeldt, 1992. A critical review of data on field-scale dispersion in aquifers. *Water Resour. Res.* 28:1955-1974.

Looney, B.B., M.W. Grant and C.M. King, 1987. Estimation of geochemical parameters for assessing subsurface transport at the Savannah River Site DPST-85-904. E.I. du Pont de Nemours & Co.

Melamed, R., J.J. Jurinak and L.M. Dudley, 1994. Anion exclusion-pore velocity interaction affecting transport of bromide through an oxisol. *Soil Sci. Soc. Am. J.* 58:1405-1410.

Neuweiler, I., S. Attinger and W. Kinzelbach, 2001. Macrodispersion in a radially diverging flow field with finite Peclet numbers 1. Perturbation theory approach. *Water Resour. Res.* 37:481-493.

Schaap, M.G., F.J. Leij and M.T. van Genuchten, 2001. ROSETTA: A computer program for estimating soil hydraulic parameters with hierarchical pedotransfer functions. *J. Hydrol.* 251:163-176.

Seaman, J.C, 1998. Retardation of fluorobenzoate tracers in highly weathered soil and groundwater systems. *Soil Sci. Soc. Am. J.* 62:354-361.

Seaman, J.C., P.M. Bertsch and D.I. Kaplan, 2006a. Spatial and temporal variability in colloid dispersion as a function of groundwater injection rate within Atlantic Coastal Plain sediments. *Vadose Zone J.* In review.

Seaman, J.C., M. Wilson, P.M. Bertsch, J. Singer, F. Majs and S.A. Aburime, 2006b. Tracer migration in a radial flow field: Longitudinal dispersivity and anionic tracer retardation. *Vadose Zone J.* In review.

Seaman, J.C., F. Majs, J. Singer, S. Aburime and P.M. Bertsch, 2007. Analysis of tracer migration in a diverging radial flow field. *Proc. GWRC* This issue.

Šimůnek, J., M. Šejna and M.T.v. Genuchten, 1999. The HYDRUS-2D software package for simulating two-dimensional movement of water, heat, and multiple solutes in variably-saturated media. USDA ARS Salinity Lab, Riverside, CA.

Welty, C. and L.W. Gelhar, 1994. Evaluation of longitudinal dispersivity from nonuniform flow tracer tests. *J. Hydrol.* 153:71-102.

WSRC, 1992. F- and H-Area Seepage Basins Well Installations for Aquifer Injection Testing, Data Summary WSRC-RP-92-896